NATIONAL ADVISORY COMMITTEE FOR AERONAUTICS

TECHNICAL NOTE 1992

LINEARIZED LIFTING-SURFACE THEORY FOR SWEPT-BACK

WINGS WITH SLENDER PLAN FORMS

By Harvard Lomax and Max. A. Heaslet

Ames Aeronautical Laboratory
Moffett Field, Calif.

NACA

Washington

December 1949

NATIONAL ADVISORY COMMITTEE FOR AERONAUTICS

TECHNICAL NOTE 1992

LINEARIZED LIFTING-SURFACE THEORY FOR SWEPT-BACK

WINGS WITH SLENDER PLAN FORMS

By Harvard Lomax and Max. A. Heaslet

SUMMARY

The spanwise and chordwise distribution of loading, the lift, and the induced drag of a swept-back wing of slender plan form are developed by means of linearized lifting-surface theory. The results are applicable for all free-stream Mach numbers. The term slender implies that the ratio of the reduced span (equal to the product of $|1 - (\text{Mach number})^2|^{1/2}$ and the span) to the over-all length of the wing is small.

INTRODUCTION

Theoretical linearized solutions for the distribution of loading over lifting surfaces traveling at subsonic or supersonic speeds can be separated into two classes. One, in which the loading is given and the twisted surface required to support such a loading is found, can be expressed mathematically in a form necessitating the evaluation of a double integral involving doublets of prescribed intensity scattered over the plan form of the wing. The other, and usually more difficult problem, in which the shape of the surface is specified and the resulting loading is to be determined, can be resolved into the problem of solving a double integral equation involving doublets of unknown intensity scattered over the wing plan form. It is this latter type of problem, sometimes referred to as a problem of the second kind, with which this paper is to be particularly concerned.

In subsonic studies these double integral equations have been avoided by use of the lifting-line theory introduced by Prandtl. This simplification reduces the analysis of three-dimensional loading problems to the study of a single integral equation more susceptible to analysis. In supersonic studies, on the other hand, many important types of wing plan forms can be completely analyzed without further simplification. Outstanding examples of such plan forms are those in which the methods of conical flow can be used. Effectively, the presence of a conical flow field reduces the problem one order dimensionally so that again only a single integral equation remains to be solved. There is yet another type of flow pattern that will reduce the double to the single

integral equation and it is proposed now to exploit this phase of the linearized lifting—surface problem.

The basic linearized partial differential equation for the per—turbation velocity potential Φ in subsonic and supersonic flow is known to be

$$(1-M_o^2)\ \Phi_{XX} + \Phi_{YY} + \Phi_{ZZ} = 0 \qquad (1)$$

where M_o is the Mach number of the free stream directed parallel to the positive X axis. Conditions sufficient to obtain this equation from the more general equation based on the assumption of a perfect gas in nonviscous, compressible, irrotational flow are that the induced velocities and the nondimensional velocity gradients are small. None of these restrictions explicitly excludes the study of equation (1) when the free—stream Mach number is set equal to unity and, in fact, for wings with swept—back plan forms, solutions to equation (1) with $M_o=1$ can be obtained that do not violate the assumptions needed to linearize the equation. In this case the first term of the equation vanishes. There are, moreover, many applications of equation (1) to aerodynamic problems in which the free—stream gradient of velocity Φ_{XX} is itself small as compared to the velocity gradients in the other directions. Such is the usual case when the wing plan form is long and slender, that is, when the length of the wing is large in terms of the span. In this case, also, the first term of equation (1) may be neglected.

It is possible and even preferable to combine the two conditions involving, in the one case, the free—stream Mach number and, in the other, the wing geometry into one condition that will be satisfied by both or either of the two. This can be done by considering the Mach number effect to be a stretching factor which elongates distances in the X direction as the Mach number approaches unity. In this sense a slender wing is one for which $\dfrac{\sqrt{1-M_o^2}\ \times\ \text{span}}{\text{length}}$ is small and the theory in this report is valid for all such slender wings.

It does not matter, then, whether $M \approx 1$ or whether the chordwise gradients are comparatively small; in either case equation (1) reduces to

$$\Phi_{YY} + \Phi_{ZZ} = 0 \qquad (2)$$

which is simply Laplace's equation for the perturbation velocity potential in a transverse plane.

Since slender wings and slender wing—body combinations are of increasing practical importance, and since the assumption of slenderness

together with the simplicity embodied in equation (2) permits the study
of relatively complex aerodynamic configurations, a number of investi-
gations based upon the resultant methods have already been published.
In reference 1 low-aspect-ratio wings were studied and references 2, 3,
4, and 5 included, respectively, a complete analysis of all the stability
derivatives of a low-aspect-ratio triangular wing, a lifting triangular
wing with an arbitrary body of revolution, a lifting triangular cruciform
combination on an arbitrary body of revolution, and damping-in-roll
calculations for slender swept-back wings and slender wing-body combina-
tions. In references 6 and 7 the load distribution, the lift, and the
drag were calculated for slender swept-back wings with straight leading
edges and with tips cut normal to the free-stream direction. The object
of the present report is to generalize, as far as possible, the plan
forms amenable to slender wing analysis. Thus, leading edges of rather
arbitrary shape are included and particular attention is given to the
effect of tip shape on the load distribution. The aerodynamic charac-
teristics of two families of plan forms will also be included.

A list of the important symbols used is given in the appendix.

ANALYSIS

The means of satisfying boundary conditions for Laplace's equation
are classical in nature and only a sketch of the developments to be used
need be given here. The boundary conditions for a lifting surface
without thickness are:

1. Perturbation velocities vanish at infinity

2. For all points on the $Z=0$ plane and not on the wing or its
vortex sheet

$$\Delta\Phi = \Phi_{Z=0+} - \Phi_{Z=0-} = 0$$

3. For all points on the $Z=0$ plane

$$\Delta\frac{\partial\Phi}{\partial Z} = \left(\frac{\partial\Phi}{\partial Z}\right)_{Z=0+} - \left(\frac{\partial\Phi}{\partial Z}\right)_{Z=0-} = 0$$

4. For all points on the $Z=0$ plane, within the boundaries of the
plan form, $\left(\frac{\partial\Phi}{\partial Z}\right)_{Z=0}$ is specified

Applying these conditions together with the two-dimensional form of Green's theorem, it is possible to express (see, for example, reference 7) the general solution of equation (2) in the form[1]

$$\Phi(X,Y,Z) = \frac{Z}{2\pi} \int_{-S(X)}^{S(X)} \frac{\Delta\Phi(X,Y_1)dY_1}{(Y-Y_1)^2+Z^2}$$
(3a)

where $Y=S(X)$ denotes the local semispan of the wing. If the wing has a straight leading edge and if θ is the semiapex angle, then

$$S(X) = X \tan \theta$$

In all cases the semispan of the wing will be denoted S_O.

At this point in the analysis a convenient change in notation can be introduced. Distances in the X direction are divided by the root chord C_r while distances in the Y and Z directions are divided by the product of C_r and the tangent of the semiapex angle. Nondimensional variables x,y,z are thus determined such that

$$x = \frac{X}{C_r} \, , \quad y = \frac{Y}{C_r \tan \theta} \, , \quad z = \frac{Z}{C_r \tan \theta}$$

while at the same time, by definition,

$$\Phi(X,Y,Z) = \Phi(xC_r, \, yC_r \tan \theta, \, zC_r \tan \theta) = \varphi(x,y,z)$$

and

$$S(X) = S(xC_r) = s(x) \, C_r \tan \theta$$

---

[1]Equation (3a) is valid provided no point exists within or on the boundaries of the flow field such that

$$\lim_{\epsilon \to 0} \epsilon \frac{\partial \Phi}{\partial \epsilon} \neq 0$$

where ϵ is the radial distance from the point.

Perturbation velocities in physical space will be denoted conventionally by u, v, w; hence

$$\frac{\partial \Phi}{\partial X} = u \ , \ \frac{\partial \Phi}{\partial Y} = v \ , \ \frac{\partial \Phi}{\partial Z} = w$$

In the transformed variables

$$\frac{\partial \phi}{\partial x} = u C_r \ , \ \frac{\partial \phi}{\partial y} = v C_r \tan \theta \ , \ \frac{\partial \phi}{\partial z} = w C_r \tan \theta$$

No ambiguity should arise if u, v, w are used as functional symbols for velocity components in either set of coordinate systems; thus u(X,Y,Z) transforms into u(x,y,z).

Equation (3a) now becomes

$$\phi(x,y,z) = \frac{z}{2\pi} \int_{-s(x)}^{s(x)} \frac{\Delta\phi(x,y_1)dy_1}{(y-y_1)^2+z^2} \tag{3b}$$

and this can be put in a more useful form by integrating by parts. Thus, since φ must be a continuous function of z everywhere except on the lifting surface and on the trailing vortex sheet,

$$\Delta\phi(-s) = \Delta\phi(s) = 0$$

and equation (3b) becomes

$$\phi = \frac{C_r \tan \theta}{2\pi} \int_{-s}^{s} \Delta v \ \mathrm{arc} \tan \left(\frac{y-y_1}{z} \right) dy_1 \tag{4}$$

where v is the perturbation velocity component in the Y direction and Δv is the jump in the value of v in the XY plane. Since, moreover, s and Δv are not functions of z, the derivative of both sides of equation (4) with respect to z leads to the result

$$w = -\frac{1}{2\pi} \int_{-s}^{s} \frac{y-y_1}{(y-y_1)^2+z^2} \Delta v \ dy_1$$

which as z approaches zero reduces to the final form

$$w_{z=0} = w_0 = - \frac{1}{2\pi} \int_{-s(x)}^{s(x)} \frac{\Delta v(x, y_1) dy_1}{y - y_1} \quad , \quad - s < y < s \qquad (5)$$

Equation (5) is sometimes referred to as Prandtl's integral equation.

Interest is now fixed on the class of problems for which the streamwise slope λ of the surface is given. Vertical induced velocity w_0 and λ satisfy the relation

$$\lambda(X, Y) = \frac{w_0}{V_0} \qquad (6)$$

which simply states that the lifting surface is along a stream plane. The approximation has been made, of course, in equation (6) that the local slope of the airfoil is the same as the slope of the streamline passing through the Z=0 plane at the same values of X and Y, an approximation usual in thin airfoil problems and consistent with the linearization of the partial differential equation if the slopes are small. Combining equation (6) with equation (5) permits the study of a swept-back wing of arbitrary twist and angle of attack. The case of greatest practical interest, however, is the one in which the lifting surface is a flat plate at a constant angle of attack; for this case w_0 is independent of X and Y.

Solutions of the integral equation given by equation (5) are well known in the studies of aerodynamic problems. (See, e.g., references 8, 9, and 10.) If the restriction is made that

$$\int_{-s}^{s} \Delta v(y) dy = 0$$

then equation (5) can be inverted to the form

$$\Delta v = \frac{2}{\pi} \frac{1}{(s-y)^{1/2}[y-(-s)]^{1/2}} \int_{-s}^{s} \frac{w_0(y_1)(s-y_1)^{1/2}[y_1-(-s)]^{1/2}}{y-y_1} dy_1 \qquad (7)$$

(Equation (7) and, later, equation (8) are written in a form such that they can be generalized to the case where the distance to the left edge, $-s$, does not necessarily equal the distance to the right edge, s). The solution represented by equation (7) is extremely useful in application since it insures that the jump in potential at the extreme edges is zero. However, it is by no means the most general solution to equation (5). Under the restriction

$$\int_{-s}^{s'} \frac{w_0(y)dy}{(s-y)^{1/2}[y-(-s)]^{1/2}} = 0$$

the inversion of equation (5) can also be expressed in the form

$$\Delta v = \frac{2}{\pi} (s-y)^{1/2}[y-(-s)]^{1/2} \int_{-s}^{s} \frac{w_0(y_1)dy_1}{(y-y_1)(s-y_1)^{1/2}[y_1-(-s)]^{1/2}} \quad (8a)$$

to which the additional term[2]

$$\Delta v = \frac{A_0}{(s-y)^{1/2}[y-(-s)]^{1/2}} \quad (8b)$$

can be added since this term gives zero values of w_0 in the interval $-s \leq y \leq s$ for arbitrary A_0. In the solution of aerodynamic problems the choice of A_0 is usually made by considering additional restrictions on the physical flow pattern such as the Kutta condition at the trailing edge of a lifting surface.

The solutions represented by equations (7) and (8) present sufficiently strong mathematical tools to provide for the study of a large class of swept-back plan forms. No attempt has been made here to derive the most general form of the solution. It must suffice to remark that the inversion can be accomplished through the application of conformal transformations, as was presented by Söhngen in reference 8, or through a generalization of the integral operator methods commonly used in the inversion of Abel's integral equation.

LOAD DISTRIBUTION FOR FLAT SWEPT-BACK WING

The analysis derived in the preceding section is now to be applied to the study of swept-back wings of the type shown in figure 1. The family of plan forms is drawn with straight leading edges and with tips cut off parallel to the free-stream direction since such wings are to be discussed in detail. In the determination of the properties of these

---

[2]Terms such as

$$\Delta v = \frac{B_i}{(y+\mu_i)(s^2-y^2)^{1/2}}$$

(where B_i and μ_i are arbitrary constants $(-s < \mu_i < s)$) are excluded by the condition given in footnote 1.

wings, however, it is not necessary to maintain rigid restrictions on the geometric parameters during the early stages of the analysis and, in the interest of generality, an attempt will be made to defer limitations in shape. In particular, discussion of more general types of tip boundaries will be included. The plan form, therefore, is assumed symmetrical with respect to the X axis or free-stream direction, has a semiapex angle equal to θ, has a leading edge given by the equation Y=S(X), has a trailing edge of unspecified shape, and is terminated spanwise by an arbitrary tip.

The remainder of the treatment can best be divided into three parts corresponding to the three regions shown in the figure. Thus, region 1 extends from the apex to the trailing edge of the root chord, region 2 continues streamwise to the end of the leading edge, and region 3 includes the remainder of the wing.

Region 1

In region 1 the boundary conditions in the transformed plane require w_0 to be a constant for $-s \leqq y \leqq s$. Since along the leading edge $\Delta\varphi(-s) = \Delta\varphi(s) = 0$, equation (7) provides the complete inversion and the solution can be written

$$\Delta v = \frac{2w_0 y}{[s^2(x)-y^2]^{1/2}} \tag{9a}$$

for

$$-s \leqq y \leqq s$$

or, if a straight leading edge is used,

$$\Delta v = \frac{2w_0 y}{(x^2-y^2)^{1/2}} \tag{9b}$$

for

$$-x \leqq y \leqq x$$

The jump in potential becomes

$$\Delta\varphi = C_r \tan\theta \int_s^y \Delta v \, dy_1 = -2w_0 C_r \tan\theta \, (s^2-y^2)^{1/2} \tag{10}$$

Since the loading coefficient can be written

$$\frac{\Delta p}{q} = \frac{2\Delta u}{V_0} = \frac{2}{V_0}\frac{\partial\Delta\Phi}{\partial X} = \frac{2}{V_0 c_r}\frac{\partial\Delta\varphi}{\partial x}$$

then

$$\frac{\Delta p}{q} = \frac{-4w_0 \tan\theta}{V_0}\frac{s(ds/dx)}{(s^2-y^2)^{1/2}} \qquad (11a)$$

or, for a straight leading edge,

$$\frac{\Delta p}{q} = \frac{-4w_0 \tan\theta}{V_0}\frac{x}{(x^2-y^2)^{1/2}} \qquad (11b)$$

Equations (11a) and (11b) can be transformed finally to the physical plane and, setting $\alpha = \dfrac{-w_0}{V_0}$,

$$\frac{\Delta p}{q} = \frac{4\alpha S(dS/dX)}{(S^2-Y^2)^{1/2}} \qquad (12a)$$

or, for a straight leading edge,

$$\frac{\Delta p}{q} = \frac{4\alpha X \tan^2\theta}{(X^2 \tan^2\theta-Y^2)^{1/2}} \qquad (12b)$$

These expressions have been derived in reference 1 for low-aspect-ratio wings.

Region 2

The boundary conditions in region 2 are considerably complicated by the presence of the vortex sheet lying between the trailing edges. If, as in the accompanying sketch, the trailing edge is at $\pm t(x)$, then, in a plane perpendicular to the x axis, w_0 is constant between $\pm t$ and $\pm s$, and between $-t$ and $+t$ the value of $\Delta\varphi$ is consistent with the loading on upstream sections of the wing; that is, the strength and distribution of vortices trailing from a lifting surface are proportional to the gradient of the span loading.
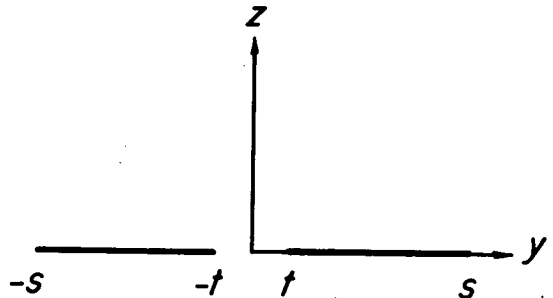
For $|y| > |s|$, $\Delta\varphi=0$ since no lifting elements occur outside the span of the wing. However, since a streamwise increase in $\Delta\varphi$ corresponds to a loading, $\Delta\varphi$ at any point behind the wing must be the same as $\Delta\varphi$ at the trailing edge for the same y. If the equation of the trailing edge is written in either of the forms

$$\left.\begin{aligned} y &= t(x) \\ x &= t^*(y) \end{aligned}\right\} \quad (13)$$

then, for $x > t^*$

$$\Delta\varphi(x,y) = \Delta\varphi(t^*,y) \qquad (14)$$

Since $\Delta\varphi(t^*,y)$ is a function of the single variable y, its derivative with respect to y may be written in the form

$$\frac{d\Delta\varphi(t^*,y)}{dy} = \frac{\partial\Delta\varphi(t^*,y)}{\partial t^*} \frac{dt^*}{dy} + \frac{\partial\Delta\varphi(t^*,y)}{\partial y}$$

But from the definition of $\frac{\Delta p}{q}$, it follows that

$$\frac{\partial\Delta\varphi(t^*,y)}{\partial t^*} = \frac{V_0 c_r}{2} \left.\frac{\Delta p}{q}\right]_{x=t^*}$$

Introducing now the notation Δv_w for Δv in the vortex wake (i.e., for $-t < y < t$) and Δv_p for the lateral induced velocity on the plan form (i.e., for $t < |y| < s$), it follows that

$$\Delta v_p = \frac{1}{c_r \tan\theta} \frac{\partial\Delta\varphi_p(x,y)}{\partial y}$$

and

$$\Delta v_w = \frac{V_0}{2\tan\theta} \left.\frac{\Delta p}{q}\right]_{x=t^*} \frac{dt^*}{dy} + \Delta v_p \Big]_{x=t^*} \qquad (15)$$

Thus the lateral induced velocity in the vortex wake is determined by the loading on the trailing edge and the value of Δv_p as the trailing edge is approached.

Using equation (5) and invoking the condition that $\Delta\varphi$ is symmetrical with respect to the x axis

$$w_0 = -\frac{1}{2\pi}\int_0^t \frac{2y_1\Delta v_w dy_1}{y^2-y_1^2} - \frac{1}{2\pi}\int_t^s \frac{2y_1\Delta v_p dy_1}{y^2-y_1^2} \tag{16}$$

Furthermore, if the Kutta condition is to hold, then the loading coefficient $\Delta p/q$ must be zero on the trailing edge and equation (15) reduces to $\Delta v_w = \Delta v_p]_{x=t^*}$. Thus, if t_1^* is written for $t^*(y_1)$ and the change in variables

$$\left.\begin{aligned}y^2 &= \eta \\ y_1^2 &= \eta_1 \\ 2y_1 dy_1 &= d\eta_1\end{aligned}\right\} \tag{17}$$

is made, equation (16) becomes

$$w_0 = -\frac{1}{2\pi}\int_0^{t^2} \frac{\Delta v_p(t_1^*,y_1)d\eta_1}{\eta-\eta_1} - \frac{1}{2\pi}\int_{t^2}^{s^2} \frac{\Delta v_p(x,y_1)d\eta_1}{\eta-\eta_1} \tag{18}$$

This is an integral equation in which w_0 is known to be a constant in the interval $t^2 < \eta < s^2$. The solution to equation (18), which corresponds to an arbitrary trailing edge, will be outlined in the discussion of the third region. Here attention will be limited to that particular solution contained in equations (7) and (8) which will make the first integral of equation (18) give zero and the second integral give $-2\pi w_0$. Such a solution is readily found in the form

$$\Delta v_p = 2w_0\left(\frac{\eta-t^2}{s^2-\eta}\right)^{1/2} \tag{19}$$

and, in subsequent developments, will prove to be of practical interest. Since $\Delta p/q$ has been assumed zero at the trailing edge, and further, since Δv_p as given by equation (19) is zero at the trailing edge, then equation (15) shows that Δv_w must be zero across the entire vortex wake. Physically, such a condition implies that the span loading is constant when $-t < y < t$ for when Δv_w is zero it follows that $\Delta\varphi_w$ does not vary with y. This fact will be useful later.

From equation (19) the value of $\Delta\varphi_p$ can be determined as

$$\frac{\Delta\varphi_p}{C_r \tan \theta} = 2w_0 \int_s^y \left(\frac{y_1^2-t^2}{s^2-y_1^2}\right)^{1/2} dy_1 \tag{20}$$

Introducing the notation[3]

$$\left.\begin{array}{l} k_0' = \dfrac{t}{s} = (1-k_0^2)^{1/2} \\[2mm] \dfrac{y_1}{s} = dn\ (k_0,u) = dn\ u \\[2mm] dy_1 = -sk_0^2\ sn\ u\ cn\ u\ du \end{array}\right\} \tag{21}$$

equation (20) becomes

$$\frac{\Delta\varphi_p}{C_r \tan \theta} = -2w_0sk_0^2 \int_0^{F(\psi_0,k_0)} cn^2\ u\ du$$

so that finally

$$\frac{\Delta\varphi_p}{C_r \tan \theta} = -2w_0s\ [E(\psi_0,k_0) - k_0'^2\ F(\psi_0,k_0)] \tag{22}$$

where the elliptic integrals are defined as follows:

$$E(\psi_0,k_0) = \int_0^{\psi_0} (1-k_0^2\ \sin^2 x)^{1/2}\ dx$$

$$F(\psi_0,k\ ) = \int_0^{\psi_0} \frac{dx}{(1-k_0^2\ \sin^2 x)^{1/2}}$$

---

[3]The notation on elliptic functions is taken from Whittaker and Watson (reference 11) except for the use of $F(\psi,k)$ which can be found more readily in tabulated form.

the argument ψ_0 is

$$\psi_0 = \text{arc sin } \left(\frac{s^2-y^2}{s^2-t^2}\right)^{1/2} \qquad (23)$$

and the modulus k_0 is given by equation (21). It will be noted that, when t is zero, equation (22) reduces to equation (10). That is, $\Delta\varphi$ is continuous in passing from region 1 to region 2. This condition is, of course, essential.

The loading coefficient on the wing plan form can now be found from equation (22) through use of the relation

$$\frac{\Delta p}{q} = \frac{2}{V_0 c_r} \frac{\partial \Delta\varphi}{\partial x}$$

In this way

$$\frac{\Delta p}{q\alpha \tan \theta} = 4 \frac{ds}{dx} \left[E(\psi_0, k_0) + \frac{y}{s} \left(\frac{y^2-t^2}{s^2-y^2}\right)^{1/2} \right] - 4k_0' \frac{dt}{dx} F(\psi_0, k_0) \qquad (24)$$

Again, when t is set equal to zero, the loading coefficient becomes that given by equation (11a). This continuity in pressure between regions 1 and 2 is by no means essential; in fact it will be seen later that in passing from region 2 to region 3 an abrupt discontinuity in pressure occurs.

In deriving equation (18) the Kutta condition was assumed to hold at the trailing edge. This condition has yet to be applied to the expression for the loading coefficient in region 2 (equation (24)). So far, the leading and trailing edges have been expressed in arbitrary form. The restriction to a straight leading edge is now made and the trailing edge will be determined by first setting $y=t$ and $\Delta p/q=0$ in equation (24) and then solving for t as a function of x. This operation gives

$$\frac{dt}{dx} = \frac{E_0}{K_0 k_0'} \qquad (25)$$

where

$$E_0 = E\left(\frac{\pi}{2}, k_0\right), \quad K_0 = F\left(\frac{\pi}{2}, k_0\right)$$

and dt/dx is, of course, the slope of the trailing edge. The solution

to this equation that satisfies the condition x=1 when t=0 can be
written in the form

$$t = \frac{k_0'}{E_\sigma - k_0'^2 K_0} \qquad (26)$$

That this is a solution of equation (25) can be verified by direct
substitution. Actually, however, the solution was obtained from
equation (22) when the condition already mentioned that the span loading
should be constant between the trailing edges was applied. Equation
(26) gives t(x) explicitly as a function of the ratio t/x from which
a graph of the trailing edge can readily be found (fig. 2). Since
k_0'=t/x, equation (26) may be written in the form

$$x = \frac{1}{E_\sigma - k_0'^2 K_0} \qquad (26a)$$

From this form the asymptotic behavior of the trailing edge can be
deduced, since x approaches infinity as k_0' approaches unity. Hence
the trailing edge approaches asymptotically a straight line with unit
slope, that is, becomes parallel to the leading edge.

The asymptotic value of the chord is equal in magnitude to x-t as
x becomes large. When equations (26) and (26a) are used, it follows
that

$$x-t = \frac{1-k_0'}{E_\sigma - k_0'^2 K_0}$$

which is indeterminate at $k_0=0$. An application of L'Hospital's rule
gives, however,

$$(x-t)_{x \to \infty} = \frac{2}{\pi}$$

This value is shown as an asymptote in figure 2.

The solution in region 2 for the jump in potential (equation (22))
and the loading coefficient (equation (24)) have thus been shown to
apply to a wing plan form closely resembling a swept-back constant-chord
wing except that at the root chord the trailing edge is smoothly
filleted — a plan form of quite practical design. (Figs. 1(a) and 1(b)
were drawn with a trailing edge given by equation (26).) The loading
coefficient in X,Y,Z space on a plan form with a trailing edge given by
equation (26) can be written in the form

$$\frac{\Delta p}{q\alpha} = 4 \tan \theta \left\{ E(\psi_0,k_0) + \frac{Y}{X \tan \theta} \left[\frac{Y^2 - T^2(X)}{X^2 \tan^2 \theta - Y^2} \right]^{1/2} - \frac{E_0}{K_0} F(\psi_0,k_0) \right\} (27)$$

$$k_0 = \left[1 - \frac{T^2(X)}{X^2 \tan^2 \theta} \right], \quad \psi_0 = \text{arc sin} \left[\frac{X^2 \tan^2 \theta - Y^2}{X^2 \tan^2 \theta - T^2(X)} \right]^{1/2}$$

where $T(X) = t(x) C_r \tan \theta$ is the ordinate of the trailing edge (fig. 1(a)) and can be determined in general from equation (26) for a given wing geometry and a value of X. The first part of this variation for $0 \leqq t(x) \leqq 1.2$ is shown in figure 2.

When the wing aspect ratio becomes very large, the loading on the outboard section should approach that of a two-dimensional wing, making an angle θ with the X axis. Simple sweep theory (see, e.g., reference 12) gives for the two-dimensional case the formula

$$\frac{\Delta p}{q\alpha} = \frac{4 \tan \theta}{(1 - \beta^2 \tan^2 \theta)^{1/2}} \left(\frac{C_n - X_n}{X_n} \right)^{1/2}$$

where C_n is the chord and X_n is a distance, both measured normal to the leading edge, and $\beta^2 = |1 - M_0^2|$. For small values of $\beta \tan \theta$, that is, under the assumptions of slender wing theory, this becomes

$$\frac{\Delta p}{q\alpha} = 4 \tan \theta \left(\frac{C_n - X_n}{X_n} \right)^{1/2}$$

It remains to compare the asymptotic behavior of equation (27) far outboard along the wing. To this end, a change is made to the coordinate system (see accompanying sketch) and expressed through the transformations
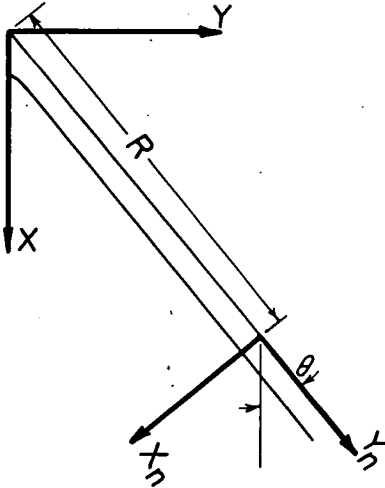
$$X = Y_n \cos \theta + X_n \sin \theta + R \cos \theta$$

$$Y = Y_n \sin \theta - X_n \cos \theta + R \sin \theta$$

It is known, however, from the previous discussion of the asymptotic value of the chord that, for large values of X, $T(X)$ approaches the value $(X-C_\infty) \tan \theta$ where C_∞ is the value of the chord at infinity and k_0 approaches zero. Hence, as R becomes large,

$$E(\psi_0, 0) = F(\psi_0, 0)$$

and in the limit

$$\left(\frac{\Delta p}{q \alpha} \right)_{R \to \infty} = 4 \tan \theta \left(\frac{C_\infty \sin \theta - X_n}{X_n} \right)^{1/2}$$

which is in complete agreement with the result previously obtained from simple sweep theory.

Region 3

In the initial portion of the following analysis the outer boundary of the wing will be considered a function of X, thus

$$Y = S(X)$$

or

$$y = s(x)$$

where

$$s(x) = \frac{S(X)}{C_r \tan \theta}$$

This will serve two purposes: Not only will the method be given for
finding the solution to different tip shapes, but also means whereby
the trailing edge in region 2 can be modified will be made evident.

When the discussion is confined to region 3, the part of the plan
form affected by the geometrical form of the tips (see fig. 1), it will
be assumed that the tips are not raked in, that the trailing edge in
region 2 is given by equation (26), and that the leading edge in region
2 is a straight line. Aside from the restriction just mentioned that
raked—in tips are excluded, the shapes of both edges in region 3 are
for practical purposes arbitrary. An extension to the raked—in case
will be given in the section on vortex drag at which time the variation
of downwash in the wake is calculated.

General solution.— The initial stages of setting up the problem are
identical to those used in region 2. Again the Kutta condition is
applied at the trailing edge and equation (18) still applies. Suppose,
now, that Δv_p consists of two parts such that

$$\Delta v_p = \Delta v_1 + \Delta v_2 \tag{28}$$

and set

$$\Delta v_1 = [2w_0 + 2g(x)] \left(\frac{\eta - t^2}{s^2 - \eta}\right)^{1/2} \tag{29}$$

If $\Delta v_2(x,y)$ and $g(x)$ were both zero, this would lead to the loading
coefficient given by equation (24) which becomes, along the trailing
edge $y = t(x)$,

$$\left(\frac{\Delta p}{q\alpha \tan \theta}\right)_1 = 4 \frac{ds}{dx} E_0 - 4 k_0' \frac{dt}{dx} K_0 \tag{30}$$

where

$$K_0 = F\left(\frac{\pi}{2}, k_0\right), \quad E_0 = E\left(\frac{\pi}{2}, k_0\right)$$

and

$$k_0' = \frac{t}{s}, \quad k_0^2 + k_0'^2 = 1$$

In this case, however, we are considering some specific plan form so that
both t and s are fixed geometrically. Although in region 2 a differ-
ential equation was set up for $t(x)$ in terms of $s(x)$ based on the
condition that loading on the trailing edge vanishes, with the boundaries
specified the loading in equation (30) must be considered as a residue

to be destroyed by the proper choice of $\Delta v_2(x,y)$ and $g(x)$. Operating on equation (28) to find the pressure at the trailing edge and applying the Kutta condition leads to the condition

$$\lim_{y \to t} \frac{\partial}{\partial x} \int_s^y \Delta v_2(x,y_1)dy_1 = 2(w_0+g) \left(\frac{ds}{dx} E_0 - k_0' \frac{dt}{dx} K_0 \right) +$$

$$4ts \frac{dg}{dt^2} \frac{dt}{dx} (E_0 - k_0'^2 K_0) \tag{31}$$

and Δv_p must, of course, satisfy equation (18) so that a further condition is supplied in the form

$$\frac{1}{2\pi} \int_{t_0^2}^{t^2} \frac{\Delta v_2(t_1^*,y_1)d\eta_1}{\eta - \eta_1} - g(x) = -\frac{1}{2\pi} \int_{t^2}^{s^2} \frac{\Delta v_2(x,y_1)d\eta_1}{\eta - \eta_1} \tag{32}$$

where t_0, as shown in figure 1, is the distance, measured parallel to the y axis, from the x axis to the trailing edge in the plane which divides region 2 and region 3.

Equation (32) can now be inverted by the use of equation (8a), provided

$$\int_{t^2}^{s^2} \frac{d\eta}{(s^2-\eta)^{1/2}(\eta-t^2)^{1/2}} \left[\frac{1}{2\pi} \int_{t_0^2}^{t^2} \frac{\Delta v_2(t_1^*,y_1)d\eta_1}{\eta - \eta_1} - g \right] = 0$$

that is, provided

$$g(x) = \frac{1}{2\pi} \int_{t_0^2}^{t^2} \frac{\Delta v_2(t_1^*,y_1)d\eta_1}{(s^2-\eta_1)^{1/2}(t^2-\eta_1)^{1/2}} \tag{33}$$

Applying the inversion and using this condition for g(x)

$$\Delta v_2 = \frac{1}{\pi^2} \int_{t^2}^{s^2} \frac{d\eta_2}{\eta-\eta_2} \left[\frac{(s^2-\eta)(\eta-t^2)}{(s^2-\eta_2)(\eta_2-t^2)} \right]^{1/2} \int_{t_0^2}^{t^2} \left[\frac{1}{\eta_2-\eta_1} - \frac{1}{(s^2-\eta_1)^{1/2}(t^2-\eta_1)^{1/2}} \right] \Delta v_2(t_1^*,y_1)\,d\eta_1$$

which can be simplified (remembering that $t^2 < \eta < s^2$) to the form

$$\Delta v_2 = \frac{1}{\pi} \int_{t_0^2}^{t^2} \frac{\Delta v_2(t_1^*,y_1)\,d\eta_1}{\eta-\eta_1} \left[\frac{(s^2-\eta)(\eta-t^2)}{(s^2-\eta_1)(t^2-\eta_1)} \right]^{1/2} \qquad (34)$$

This expression placed in equation (31) yields for the left-hand side of the equation, since $\Delta v_2(x,s)=0$ by equation (34),

$$\frac{1}{\pi} \int_s^t -dy\, \frac{\partial}{\partial x} \int_{t_0^2}^{t^2} \frac{\Delta v_2(t_1^*,y_1)\,d\eta_1}{\eta-\eta_1} \left[\frac{(s^2-\eta)(\eta-t^2)}{(s^2-\eta_1)(t^2-\eta_1)} \right]^{1/2}$$

It can be shown that $\Delta v_2(t_1^*,y_1)=0$ at $y_1=t_0$. Then integrating by parts and moving the partial derivative through the second integral gives, for the left-hand side of equation (31),

$$-\frac{2}{\pi} \int_s^t dy \int_{t_0^2}^{t^2} \frac{d\Delta v_2(t_1^*,y_1)}{d\eta_1} \frac{\partial}{\partial x} \tan^{-1} \left[\frac{(\eta-t^2)(s^2-\eta_1)}{(s^2-\eta)(t^2-\eta_1)} \right]^{1/2} d\eta_1$$

Upon reversing the order of integration, the entire equation (31) becomes

$$\frac{1}{\pi k_0^2} \int_{t_0^2}^{t^2} \int \frac{d\Delta v_2(t_1^*,y_1)}{d\eta_1} \left\{ \frac{\left[\frac{ds}{dx}(k_0'^2 K_0 - E_0)s^2 k_0'^2 + k_0's^2\frac{dt}{dx}(E_0 - K_0)\right]}{(s^2-\eta_1^2)^{1/2}(t^2-\eta_1^2)^{1/2}} - \eta_1 \frac{\left[\frac{ds}{dx}(k_0'^2 K_0 - E_0) + k_0'\frac{dt}{dx}(E_0 - K_0)\right]}{(s^2-\eta_1^2)^{1/2}(t^2-\eta_1^2)^{1/2}} \right\} d\eta_1$$

$$= (w_0+g)\left(\frac{ds}{dx}E_0 - k_0'\frac{dt}{dx}K_0\right) + 2ts\frac{dg}{dt^2}\frac{dt}{dx}(E_0 - k_0'^2 K_0) \tag{35}$$

Equation (35) is valid for arbitrary leading and trailing edges when applied to the entire region of the wing affected by a trailing edge for which the Kutta condition holds. When region 3 is to be analyzed, equation (35) is valid for arbitrary trailing edges and raked-out leading edges provided the leading and trailing edges in region 2 are the particular curves developed in the discussion of region 2 (i.e., a straight leading edge and a trailing edge given by equation (26)).

Solution for straight tip.— Equation (35) is now to be solved for the special values $s=s_0=$constant and t as given by equation (26). Using these values,

$$\int_{t_0^2}^{t^2} \frac{h(\eta_1)d\eta_1}{(t^2-\eta_1^2)^{1/2}} = f(t^2) \tag{36}$$

where

$$f(t^2) = -\frac{\pi k_1^2}{E_1-K_1}\left[(w_0+g)K_1 - \frac{2ts_0}{k_1'}\frac{dg}{dt^2}(E_1-k_1'^2 K_1)\right] \tag{37}$$

$$h(\eta_1) = (s_o^2 - \eta_1)^{1/2} \frac{d\Delta v_2(t_1^*, y_1)}{d\eta_1} \tag{38}$$

and

$$k_1' = \frac{t}{s_o}$$

Equation (36) is a special form of Abel's integral equation, the unique inversion of which is

$$h(\eta_1) = \frac{1}{\pi} \frac{d}{d\eta_1} \int_{t_o^2}^{\eta_1} \frac{f(t^2) dt^2}{(\eta_1 - t^2)^{1/2}}$$

as can be shown by direct substitution.

Using the definition of $h(\eta_1)$ given by equation (38) and integrating with respect to η_1 from t_o^2 to η,

$$\Delta v_2(t^*, y) = -\frac{1}{\pi} \sqrt{s_o^2 - \eta} \int_{t_o^2}^{\eta} \frac{f(t^2) dt^2}{(t^2 - s^2) \sqrt{\eta - t^2}} \tag{39}$$

It is apparent that equation (33) is also a form of Abel's integral equation and consequently can be inverted in exactly the same manner as equation (36). Thus, since $g = 0$ when $t = t_o$, (as $\Delta v_2(t^*, y)$ vanishes when y is zero)

$$\Delta v_2(t^*, y) = 2 \sqrt{s_o^2 - \eta} \frac{d}{d\eta} \int_{t_o^2}^{\eta} \frac{g(t^2) dt^2}{\sqrt{\eta - t^2}} \tag{40}$$

Equating the two values of $\Delta v_2(t^*, y)$ given by equations (39) and (40) yields the relation

$$2 \frac{dg}{dt^2} + \frac{f(t^2)}{\pi(t^2 - s_o^2)} = 0$$

which can be written, since the expression for $f(t^2)$ is given by equation (37) and since $t^2 - s_o^2 = -k_1^2 s_o^2$,

$$2 \frac{dg}{dt^2} = \frac{w_o + g}{s_o^2 - t^2}$$

This differential equation is easily solved for g under the condition mentioned above that $g=0$ for $t=t_0$ so that

$$g = w_0 \left[\left(\frac{s_0^2 - t_0^2}{s_0^2 - t^2} \right)^{1/2} - 1 \right]$$

Placing this in equation (40), it follows that

$$\Delta v_2(t^*, y) = 2w_0 \left(\frac{\eta - t_0^2}{s_0^2 - \eta} \right)^{1/2}$$

and, if this is placed in equation (34), there results finally

$$\Delta v_2 = 2w_0 \left\{ \left(\frac{\eta - t_0^2}{s_0^2 - \eta} \right)^{1/2} - \left[\frac{(s_0^2 - t_0^2)(\eta - t^2)}{(s_0^2 - \eta)(s_0^2 - t^2)} \right]^{1/2} \right\} \tag{41}$$

The vertical induced velocity on the plan form can be now obtained by means of equation (28), thus

$$\Delta v_p = 2w_0 \left(\frac{\eta - t_0^2}{s_0^2 - \eta} \right)^{1/2} \tag{42}$$

The velocity potential is (see the development of equation (22) from equation (20))

$$\frac{\Delta \varphi_p}{C_r \tan \theta} = \int_{s_0}^{y} \Delta v_p \, dy_1 = -2w_0 s_0 [E(\psi_2, k_2) - k_2'^2 F(\psi_2, k_2)] \tag{43}$$

where

$$k_2 = \left[1 - \left(\frac{t_0}{s_0} \right)^2 \right]^{1/2}$$

$$\psi_2 = \sin^{-1} \left(\frac{s_0^2 - y^2}{s_0^2 - t_0^2} \right)^{1/2}$$

$$\left. \right\} \tag{44}$$

and, finally, since s_0 and t_0 are independent of x, the equation for the loading coefficient becomes

$$\frac{\Delta p}{q} = 0 \tag{45}$$

It should be noticed that the value of $\Delta\varphi_p$ is continuous with that given for region 2, but that the value of the loading coefficient is not.

Discussion of Results

The qualitative nature of the load distributions resulting from the application of equations (12a), (27), and (45) to a wing of triangular plan form and to two wings of swept-back plan forms is shown in figure 3. The loading in the case of the triangular wing is, of course, the same as that given in reference 1 and, in fact, differs from the exact solution of the linearized equation for arbitrary Mach number only by the factor $1/E'$ where E' is the complete elliptic integral with modulus $\sqrt{1-\beta^2 \tan^2 \theta}$. The deviation in this case can therefore be assessed accurately. The results in figures 3(b) and 3(c) can be compared in a more general manner with the load distributions for a constant-chord wing obtained in reference 13 for supersonic Mach numbers. These results, shown in figure 4, are qualitatively quite similar to those obtained by means of slender-wing theory. Across the Mach cone from the root-chord trailing edge the loading in both cases is continuous, and falls rapidly in the after portion until it reaches zero at the trailing edge of the wing. Across the Mach cone from the leading edge of the tip the loading is discontinuous and behind it the magnitude of the loading is close to zero. The principal difference between the results of the present paper and those of reference 13 appears in the position of the discontinuities, which, in slender-wing theory, occur at the Mach lines corresponding to a free-stream Mach number of unity, rather than at Mach lines determined from exact free-stream conditions.

AERODYNAMIC CHARACTERISTICS OF FLAT SWEPT-BACK WINGS

Span Loading

The span loading for the wings shown in figure 3 can best be studied in terms of the circulation function $\Gamma(Y)$. In magnitude the circulation equals the jump in the velocity potential at the trailing edge of the wing

$$\Gamma(Y) = \Delta\Phi_{T.E.} \tag{46}$$

and total lift L is expressed in the form

$$L = \int_{-S_O}^{S_O} dY \int_{L.E.}^{T.E.} \Delta p\,dX = \rho V_O \int_{-S_O}^{S_O} \Gamma(Y)\,dY \qquad (47)$$

where L.E. and T.E. stand for leading and trailing edges. Figure 5 shows the spanwise variation of Γ for the three types of plan forms shown in figure 3, each having the same wing root chord but with types (b) and (c) having larger spans. From equation (10) circulation for the type (a) wing is

$$\Gamma(Y) = 2V_O\alpha(S_O{}^2-Y^2)^{1/2} \qquad (48)$$

while for the two other cases equation (22) gives, for $0 \leqq |Y| \leqq T_O$,

$$\Gamma(Y) = 2V_O\alpha S_O \qquad (49a)$$

and, for $T_O \leqq |Y| \leqq S_O$,

$$\Gamma(Y) = 2V_O\alpha S_O[E(\psi_2,k_2) - k'_2{}^2\,F(\psi_2,k_2)] \qquad (49b)$$

where

$$\psi_2 = \text{arc sin}\left(\frac{S_O{}^2-Y^2}{S_O{}^2-T_O{}^2}\right)^{1/2}, \quad k'_2 = (1-k_2{}^2)^{1/2} = \frac{T_O}{S_O}$$

The shapes of the curves in figure 5 reveal the differences in the basic characteristics of the three wings. First, the triangular wing has an elliptic span loading and therefore will have the least induced drag for a given span of the three wings. Second, the type (b) wing has a span loading close to the elliptic and should have characteristics quite similar to the triangular wing. Third, wing (c) has the same span loading as wing (b), but at the same time has considerably more wing area. The constant span loading given in equation (49a) corresponds, of course, to the physical conditions implicit in the functional form of Δv_p as introduced in equation (19).

Lift

The lift on the three types of wings can be obtained from direct integration. Substituting from equations (48) and (49) into equation (47) it follows that

$$L = -4w_0\rho V_0(T_0 C_r \tan\theta + I_1) \tag{50}$$

where I_1 is the double integral given by

$$I_1 = S_0 \int_{T_0}^{S_0} dY \int_{0}^{\sqrt{\frac{S_0^2-Y^2}{S_0^2-T_0^2}}} k_2^2 \left(\frac{1-\xi^2}{1-k_2^2\xi^2}\right)^{1/2} d\xi \tag{51}$$

But I_1 can be evaluated by making the substitution $Y=\xi_1 S_0$ and changing the order of integration. Thus

$$I_1 = S_0^2 k_2^2 \int_0^1 d\xi \left(\frac{1-\xi^2}{1-k_2^2\xi^2}\right)^{1/2} \int_{k'_2}^{(1-k_2^2\xi^2)^{1/2}} d\xi_1$$

Integrating with respect to ξ_1 and using the Jacobian transformation $\xi=\text{sn}(u,k_2)$

$$I_1 = S_0^2 k_2^2 \frac{\pi}{4} - S_0^2 k'_2(E_2 - k'_2^2 K_2)$$

Finally, since the function Γ given by equations (48) and (49) is continuous, then at $Y=T_0$,

$$S_0(E_2 - k'_2^2 K_2) = C_r \tan\theta$$

and

$$I_1 = S_0^2 k_2^2 \frac{\pi}{4} - T_0 C_r \tan\theta \tag{52}$$

This gives for lift (equation (50))

$$\frac{L}{q} = 2\pi\alpha S_0^2 \left(1 - \frac{T_0^2}{S_0^2}\right) \tag{53}$$

If the results for lift are to be given in coefficient form, the area of the wing plan forms must be calculated. Figure 6, obtained after a numerical integration, can be used to obtain wing aspect ratio as a function of semispan for given root chord and semiapex angle. The aspect ratio A is, of course, given by

$$A = \frac{(2S_0)^2}{S}$$

where S is wing area. From equation (53), lift coefficient is expressible in the form

$$\frac{C_L}{\alpha \tan \theta} = \frac{\pi}{2} \frac{A}{\tan \theta} \left(1 - \frac{T_0^2}{S_0^2} \right) \tag{54a}$$

Equation (54a) is valid for wings of types (b) and (c) and includes type (a) as a special case. With the information given by figures 2 and 6, the value of $C_L/\alpha \tan \theta$ can be plotted against $A/\tan \theta$ for these wings as in figure 7. It should be stressed that equation (54a) holds also when T_0 is zero and reduces in that case to

$$(C_L)_{T_0=0} = \frac{\pi}{2} A\alpha \tag{54b}$$

When T_0 equals zero for the type (b) wing, the plan form is triangular and equation (54b) agrees with the result for that case in reference 1. When $T_0=0$ for the type (c) wing, the trailing edge of the root chord is behind the leading edge of the tip and, as shown in figure 7, lift coefficient is then a linear function of aspect ratio. This transition in the lift coefficient occurs at $A=2.48 \tan \theta$.

When the aspect ratio of either the type (b) or (c) wing becomes large, it approaches the value $4S_0^2 \tan \theta/(S_0^2-T_0^2)$ and the lift coefficient becomes

$$(C_L)_{A \to \infty} = 2\pi\alpha \tan \theta \tag{54c}$$

Equation (54c) corresponds to the exact expressions for lift coefficient of a swept-back infinite-aspect-ratio wing at a free-stream Mach number equal to 1 and also agrees to the first order with the low-speed lift coefficient of a highly swept, infinite-aspect-ratio wing.

Vortex Drag

The formula for the vortex drag is well known from the study of incompressible-flow theory where it is referred to as the induced drag. Its derivation for both subsonic and supersonic theory depends on the calculation of the momentum transport through a plane perpendicular to the X axis and infinitely far behind the wing.

The vortex drag of the wings under consideration can be calculated from the expression

$$D_V = - \frac{\rho C_r \tan \theta}{2} \int_{-S_0}^{S_0} (w_0)_\infty \, \Gamma dY \tag{55}$$

where $(w_0)_\infty$ is w_0 at $X = \infty$ and where, from equation (5),

$$(w_0)_\infty = - \frac{1}{2\pi} \int_{-S_0}^{S_0} \frac{(\partial \Gamma / \partial Y_1) dY_1}{Y - Y_1} \tag{56}$$

From equation (49a), for $0 \leqq |Y_1| \leqq T_0$

$$\frac{d\Gamma}{dY_1} = 0 \tag{57a}$$

and from equation (49b), for $T_0 \leqq |Y_1| \leqq S_0$

$$\frac{d\Gamma}{dY_1} = - 2V_0 \alpha \left(\frac{Y_1^2 - T_0^2}{S_0^2 - Y_1^2} \right)^{1/2} \frac{Y_1}{|Y_1|} \tag{57b}$$

Placing these expressions in equation (56), rearranging, and using the transformation $Y_1 = S_0 \sqrt{\eta_1}$, there results

$$(w_0)_\infty = \frac{V_0 \alpha}{\pi} \int_{(T_0/S_0)^{1/2}}^{1} \frac{d\eta_1}{\eta - \eta_1} \left[\frac{\eta_1 - (T_0/S_0)^2}{1 - \eta_1} \right]^{1/2} \tag{58}$$

and, after direct integration,

$$(w_0)_\infty = \begin{cases} -V_0 \alpha \left[1 - \left(\frac{T_0^2 - Y^2}{S_0^2 - Y^2} \right)^{1/2} \right] , & 0 \leqq |Y| \leqq T_0 \\ \\ -V_0 \alpha , & T_0 \leqq |Y| \leqq S_0 \end{cases} \tag{59}$$

This result is shown in the accompanying sketch for types (b) and (c)
wings and for triangular wings, the
latter being included as a special
case in the analysis when $T_0=0$.
Since the induced velocities in an
X = constant plane are a function
only of the vortices streaming through
it (equation (5)), the value of w
behind the wing is the same in every
plane. The quantity $(w_0)_\infty$, there-
fore, represents the downwash in
regions immediately behind the wing
as well as at points infinitely
distant. With this concept and the
results presented in the sketch, we
are immediately able to verify the
loading results for type (c) wings,
the loading over type (b) wings being
given, since the sketch shows that
the downwash behind the portion of
the trailing edge, which is cut normal
to the free stream, is the same as the
downwash on the wing itself. Hence,
the boundary condition that $w=w_0$ in the plane of the wing is automatically
satisfied for any variation in plan form directly behind this edge, and no
loading is required to force the streamlines into a pattern which they
already follow.
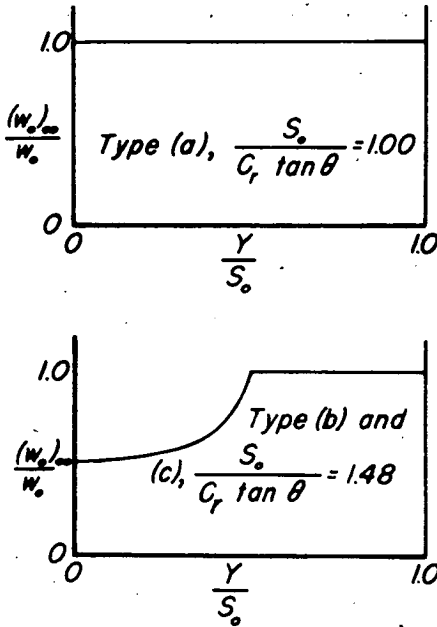
The effect of the instability and resultant rolling up of the vortex
sheet is such that the magnitude and distribution of downwash can be used
in computing induced effects off the wing only a short distance back of
the trailing edge. However, since the total kinetic energy is not
changed by this rolling up, the drag of the wing can be determined from
the velocities computed on the basis of the undistorted vortex sheet in
the XY plane. Hence, vortex drag can now be determined from equation
(55) with Γ as given in equations (49a) and (49b) and with $(w_0)_\infty$
obtained from equation (59). The expression for vortex drag then becomes

$$D_V = 2\rho V_0^2 \alpha^2 C_r \tan\theta \int_0^{T_0} \left[1 - \left(\frac{T_0^2-Y^2}{S_0^2-Y^2}\right)^{1/2}\right] dY + 2\rho V_0^2 \alpha^2 I_1$$

where I_1 has already been determined (equation (52)). The elliptic
integral can be evaluated by the transformation $Y=S_0 \, \mathrm{dn}(u,k_2)$ where,
as in equation (49b),

$$k'_2 = \frac{T_0}{S_0}$$

The final expression for drag is

$$\frac{D_v}{q\alpha^2} = S_0^2 k_2^2 \pi - 4S_0 C_r \tan\theta \; (E'_2 - k_2^2 K'_2) \tag{60}$$

where K'_2 and E'_2 are complete elliptic integrals of the first and second kind with modulus k'_2. In coefficient form, equation (60) becomes

$$\frac{C_{D_v}}{\alpha^2 \tan\theta} = \frac{A}{\tan\theta} \left(\frac{k_2^2 \pi}{4} - \frac{E'_2 - k_2^2 K'_2}{S_0/C_r \; \tan\theta} \right) \tag{61}$$

A plot of equation (61) is shown in figure 8 for all three types of wings. For large aspect ratios the vortex drag decreases as aspect ratio increases and, in fact, it can be shown that C_{D_v} approaches zero as aspect ratio becomes infinitely large. However, it is also apparent from the figure that the factor $C_{D_v}/(C_L^2/\pi A)$ increases slightly with aspect ratio in the range shown. It is the latter factor that is minimized by the elliptic span loading of the triangular wing.

Ames Aeronautical Laboratory,
National Advisory Committee for Aeronautics,
Moffett Field, Calif., Oct. 18, 1949.

APPENDIX

TABLE OF IMPORTANT SYMBOLS

A   aspect ratio of wing

C_r root chord of wing

C_L lift coefficient of wing (L/qS)

C_{D_v} vortex drag coefficient of wing (D_v/qS)

D_v vortex drag of wing

E_0, E_1 complete elliptic integrals of the second kind with moduli k_0, k_1, respectively

$E(\psi, k)$ incomplete elliptic integral of the second kind

$$\left[\int_0^\psi (1-k^2 \sin^2 x)^{1/2} \; dx \right]$$

$F(\psi,k)$ incomplete elliptic integral of the first kind

$$\left[\int_0^{\psi} \frac{dx}{(1-k^2 \sin^2 x)^{1/2}} \right]$$

$g(x)$ function introduced in equation (29)

k_0 $\left(1 - \dfrac{t^2}{s^2}\right)^{1/2} = \left(1 - \dfrac{T^2}{S^2}\right)^{1/2}$

k_1 $\left(1 - \dfrac{t^2}{s_0^2}\right)^{1/2} = \left(1 - \dfrac{T^2}{S_0^2}\right)^{1/2}$

k_2 $\left(1 - \dfrac{t_0}{s_0}\right)^{1/2} = \left(1 - \dfrac{T_0}{S_0}\right)^{1/2}$

k' $(1-k^2)^{1/2}$

K_0, K_1 complete elliptic integrals of the first kind with moduli k_0, k_1, respectively

L lift of wing

M_0 free-stream Mach number

p static pressure

q free-stream dynamic pressure $\left(\dfrac{1}{2}\rho V_0^2\right)$

$s, s(x)$ y coordinate of wing tip or wing leading edge (See fig. 1(b).) $[s(x) \ C_r \tan \theta = S(X)]$

$S(X)$ Y coordinate of wing tip or wing leading edge (See fig. 1(a).)

s_0 particular value of $s(x)$ determined by wing-tip location (See fig. 1(b).) $(s_0 \ C_r \tan \theta = S_0)$

S_0 particular value of $S(X)$ determined by wing-tip location (See fig. 1(a).)

S wing area

$t, t(x)$ y coordinate of wing trailing edge (See fig. 1(b).) $[t(x) \ C_r \tan \theta = T(X)]$

$T(X)$ Y coordinate of wing trailing edge (See fig. 1(a).)

t_O particular value of $t(x)$ determined by wing-tip location
(See fig. 1(b).) ($t_O C_r \tan \theta = T_O$)

T_O particular value of $T(X)$ determined by wing-tip location
(See fig. 1(a).)

$\left.\begin{array}{l} u(x,y,z) \\ v(x,y,z) \\ w(x,y,z) \end{array}\right\}$ transformed values of perturbation velocities in X,Y,Z direc-
tions

$\left.\begin{array}{l} u(X,Y,Z) \\ v(X,Y,Z) \\ w(X,Y,Z) \end{array}\right\}$ perturbation velocities in X,Y,Z directions

V_O free-stream velocity

$(w_O)_\infty$ vertical induced velocity at $X=\infty$, $Z=0$

x,y,z transformed Cartesian coordinates
($xC_r = X$, $yC_r \tan \theta = Y$, $zC_r \tan \theta = Z$)

X,Y,Z Cartesian coordinates in physical space

α angle of attack of wing

β $\sqrt{|1-M_O^2|}$

Γ circulation

η y^2

θ semiapex angle of wing

ρ free-stream density

$\varphi(x,y,z)$ transformed perturbation velocity potential
$[\Phi(xC_r, yC_r \tan \theta, zC_r \tan \theta)]$

$\Phi(X,Y,Z)$ perturbation velocity potential

$\dfrac{\Delta p}{q}$ loading coefficient
$\left(\dfrac{\text{pressure on lower surface} - \text{pressure on upper surface}}{q}\right)$

Δv lateral velocity discontinuities at $Z=0$

$\Delta v_1, \Delta v_2$ components of Δv_p

$\Delta \varphi$ discontinuity in perturbation potential at $z=0$

Subscripts

p   pertaining to wing plan form

w   pertaining to vortex wake

REFERENCES

1. Jones, R. T.: Properties of Low-Aspect-Ratio Pointed Wings at
      Speeds Below and Above the Speed of Sound. NACA Rep. 835, 1946.

2. Ribner, Herbert S.: The Stability Derivatives of Low-Aspect-Ratio
      Triangular Wings at Subsonic and Supersonic Speeds. NACA TN 1423,
      1947.

3. Spreiter, John R.: Aerodynamic Properties of Slender Wing-Body
      Combinations at Subsonic, Transonic, and Supersonic Speeds.
      NACA TN 1662, 1948.

4. Spreiter, John R.: Aerodynamic Properties of Cruciform-Wing and
      Body Combinations at Subsonic, Transonic, and Supersonic Speeds.
      NACA TN 1897, 1949.

5. Lomax, Harvard, and Heaslet, Max. A.: Damping-in-Roll Calculations
      for Slender Swept-Back Wings and Slender Wing-Body Combinations.
      NACA TN 1950, 1949.

6. Heaslet, Max. A., Lomax, Harvard, and Spreiter, John R.: Linearized
      Compressible-Flow Theory for Sonic Flight Speeds. NACA TN 1824,
      1949.

7. Heaslet, Max. A., and Lomax, Harvard: The Application of Green's
      Theorem to the Solution of Boundary-Value Problems in Linearized
      Supersonic Wing Theory. NACA TN 1767, 1949.

8. Söhngen, Heinz: Die Lösungen der Integralgleichung

    $$g(x) = \frac{1}{2\pi} \int_{-a}^{a} \frac{f(\xi)}{x-\xi} \, d\xi.$$ Math. Zeitschrift, V. 45, 1939, pp. 245-264.

9. von Mises, Richard, and Friedrichs, Kurt O.: Fluid Dynamics.
      Brown University Press, Providence, R. I., 1941, pp. 125-128.

10. Allen, H. Julian: General Theory of Airfoil Sections Having
      Arbitrary Shape or Pressure Distribution. NACA Rep. 833, 1945.

11. Whittaker, E. T., and Watson, G. N.: A Course of Modern Analysis.
      The University Press, Cambridge, England, 1940, 4th ed., ch. 22,
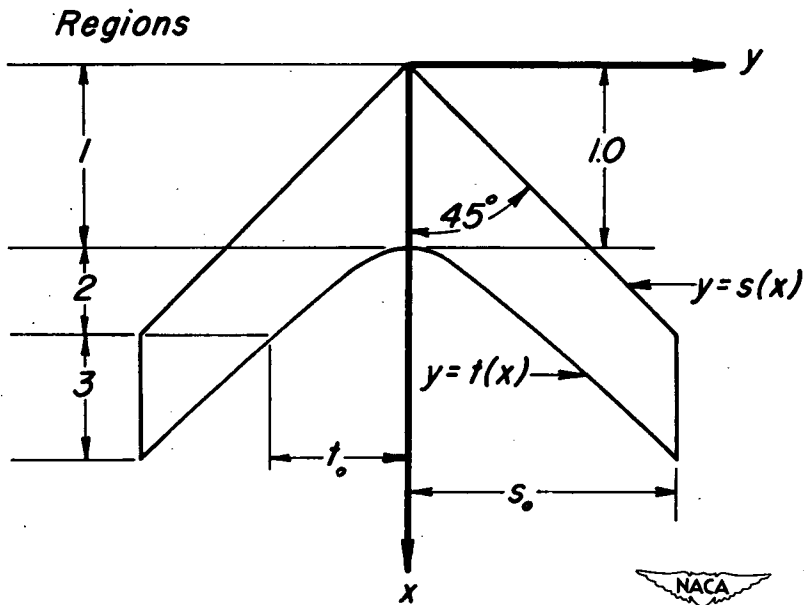   pp. 491-528.

12. Jones, R. T.: Wing Plan Forms for High-Speed Flight. NACA TN 1033,
       1946.

13. Cohen, Doris: The Theoretical Lift of Flat Swept-Back Wings at
       Supersonic Speeds. NACA TN 1555, 1948.

Page intentionally left blank

Page intentionally left blank
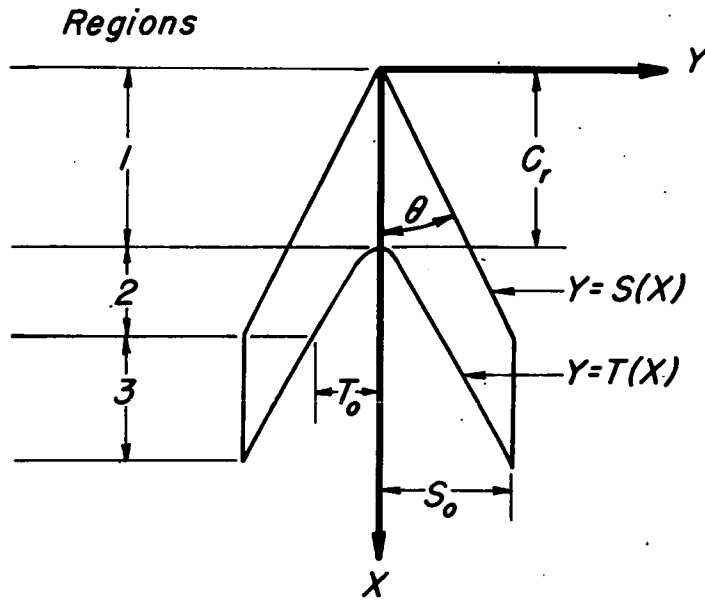
(a) Physical plane.

(b) Transformed plane.

Figure 1.— Dimensions and regions used in discussion of swept-back wings.
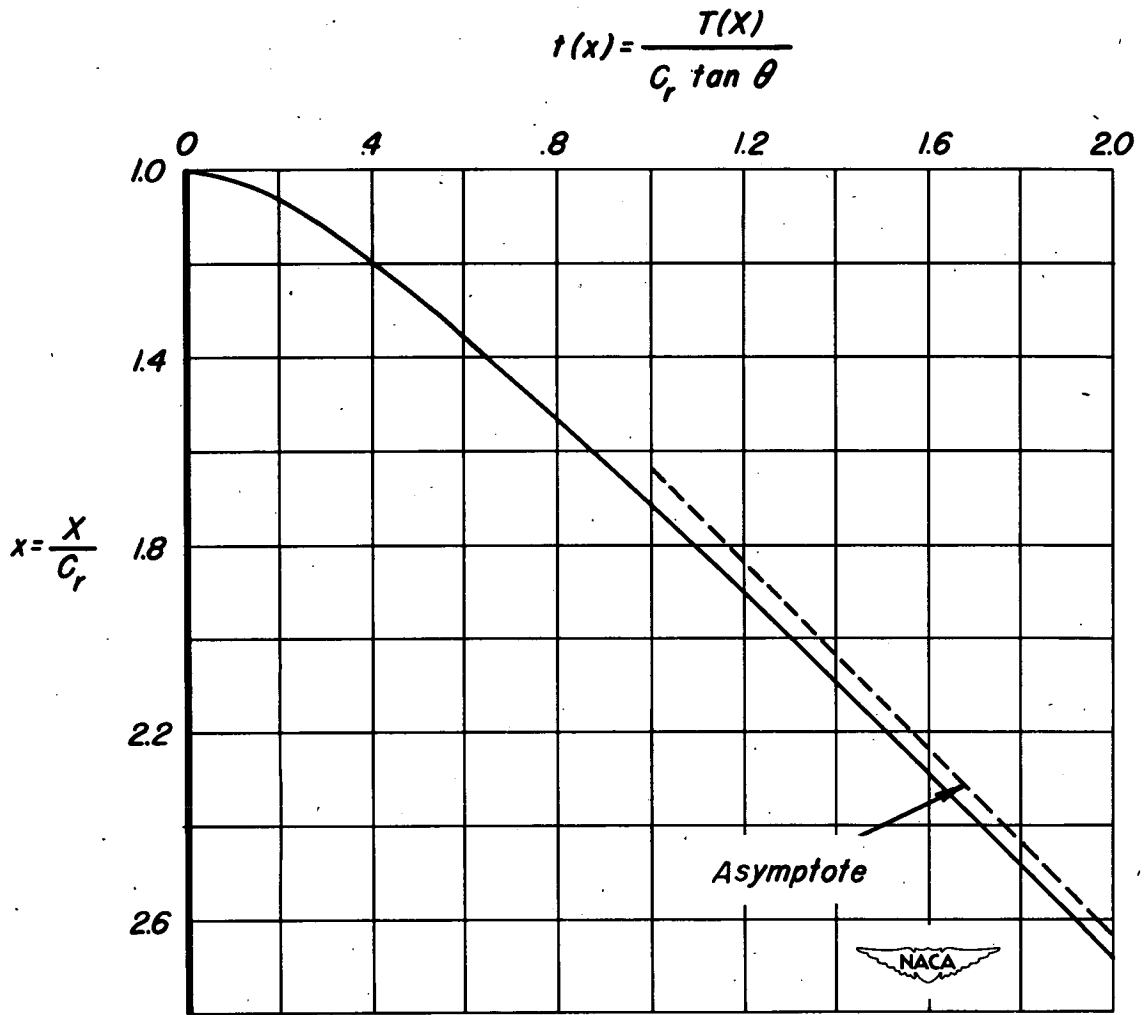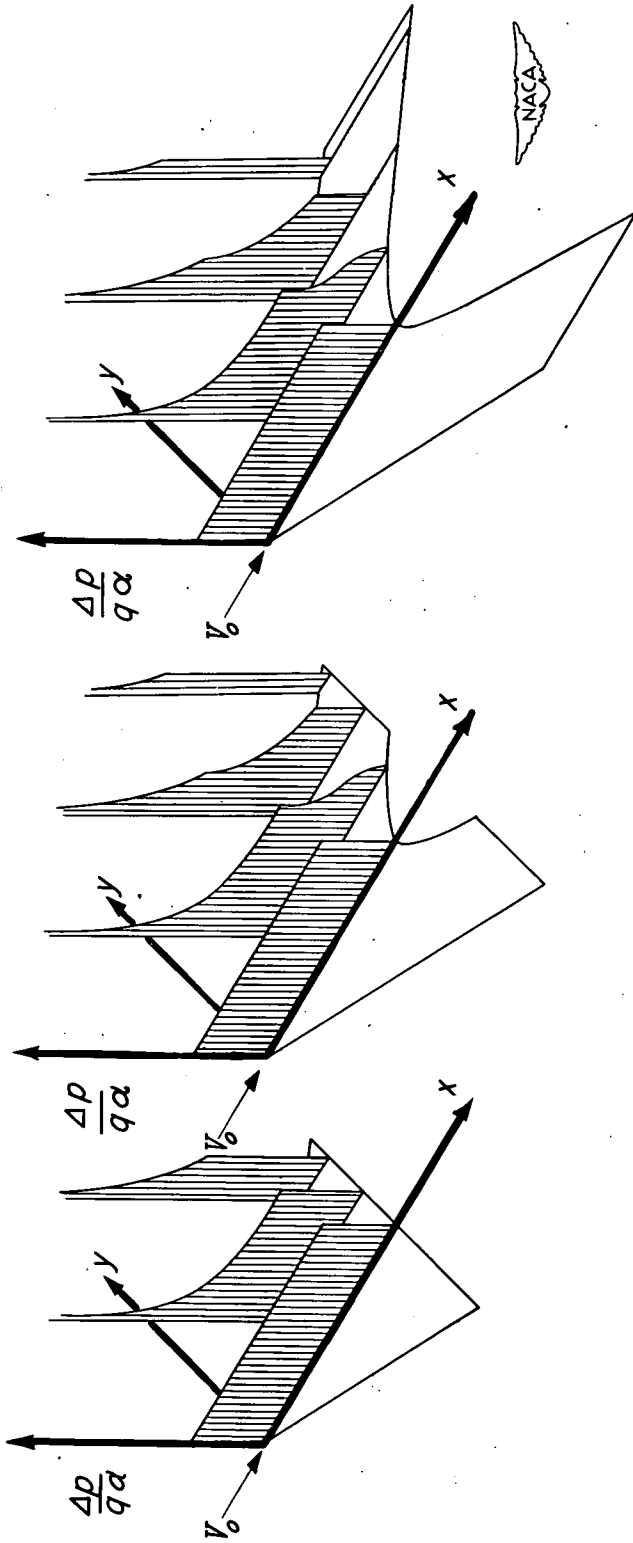
$$t(x) = \frac{T(X)}{C_r \ tan \ \theta}$$

Figure 2.– Plot showing trailing edge as given by equation (26).

(a) Triangular wing.   (b) Swept-back wing with tips   (c) Swept-back wing with tips
                              cut normal to free-stream   cut parallel to free-stream
                              direction.   direction.

Figure 3.– Load distribution from slender-wing theory for three types of pointed
          wings (transformed plane).
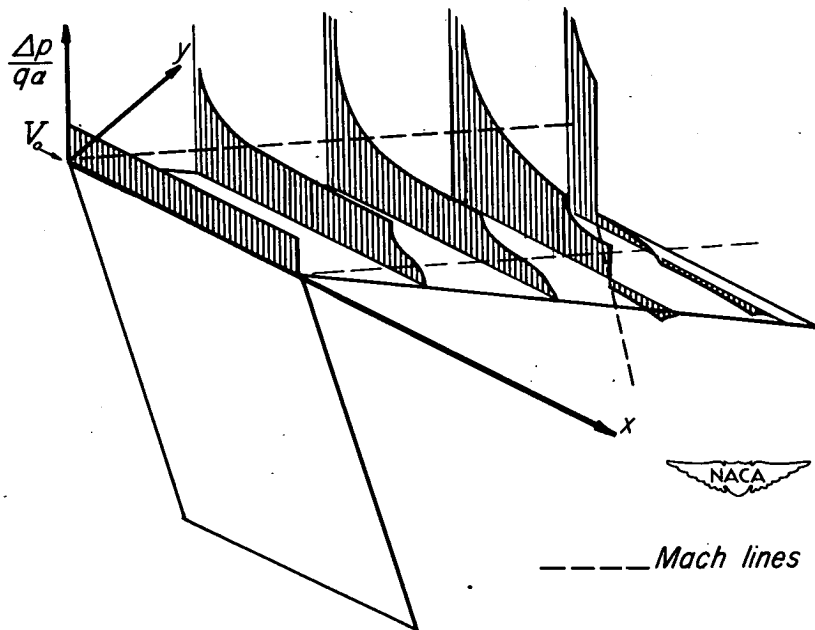
Figure 4.- Load distribution over constant-chord swept-back
wing, (reference 13).
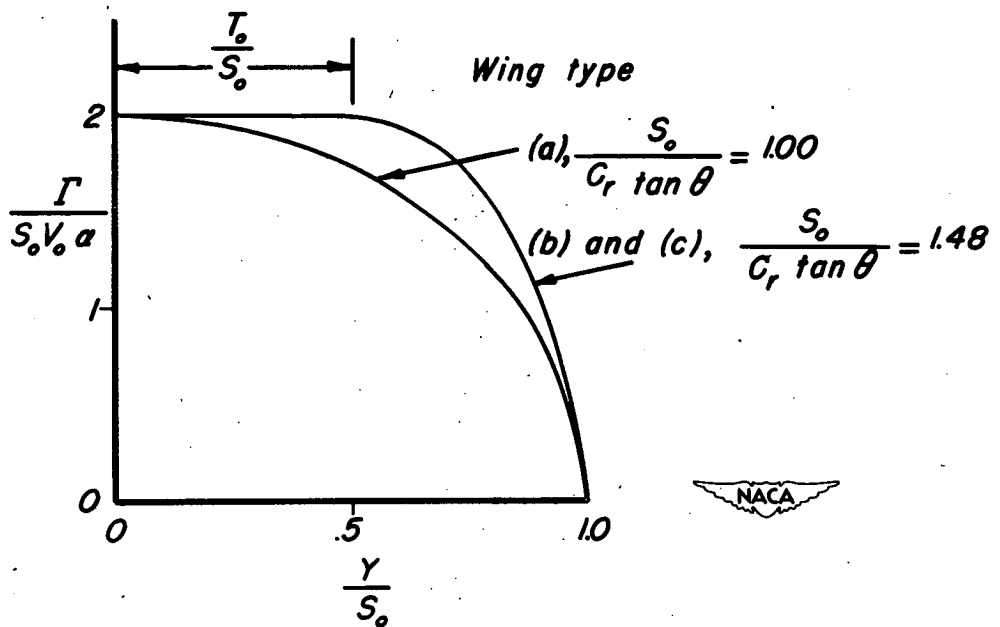
Figure 5.- Spanwise variation of section circulation for the wing plan
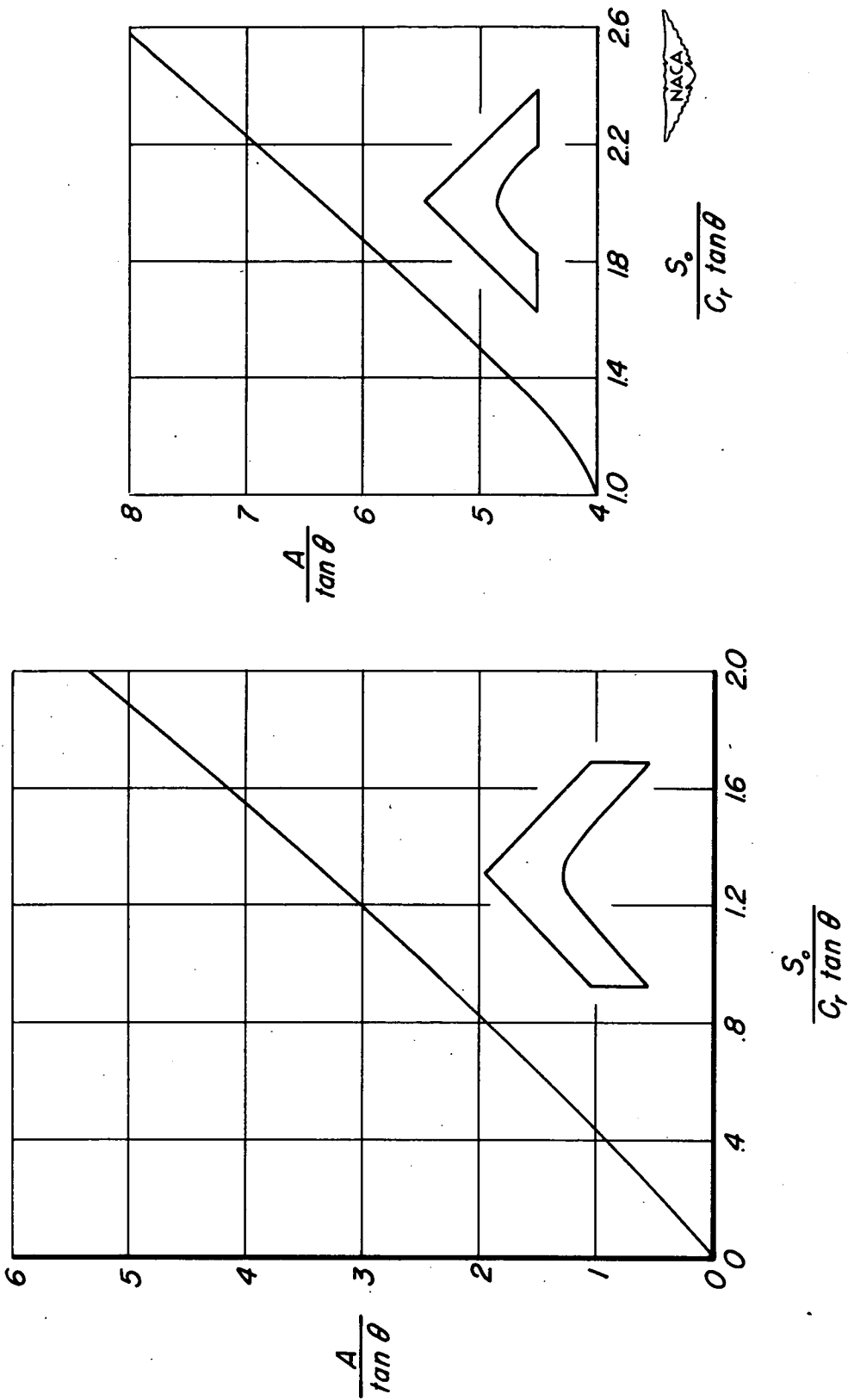forms of figure 3.

Figure 6.– Variation of aspect ratio with wing span for swept-back wings having trailing edges given by equation (26).
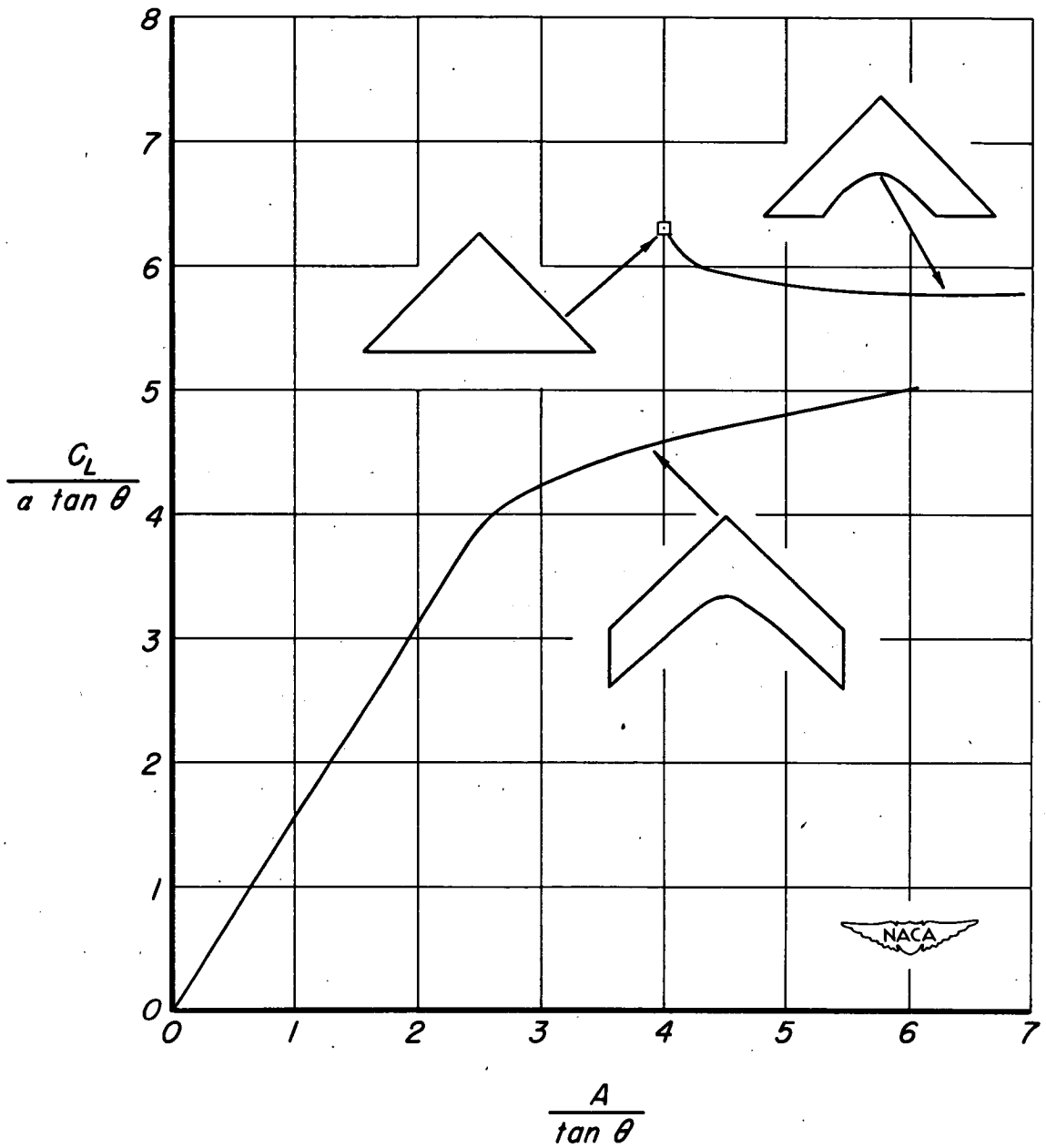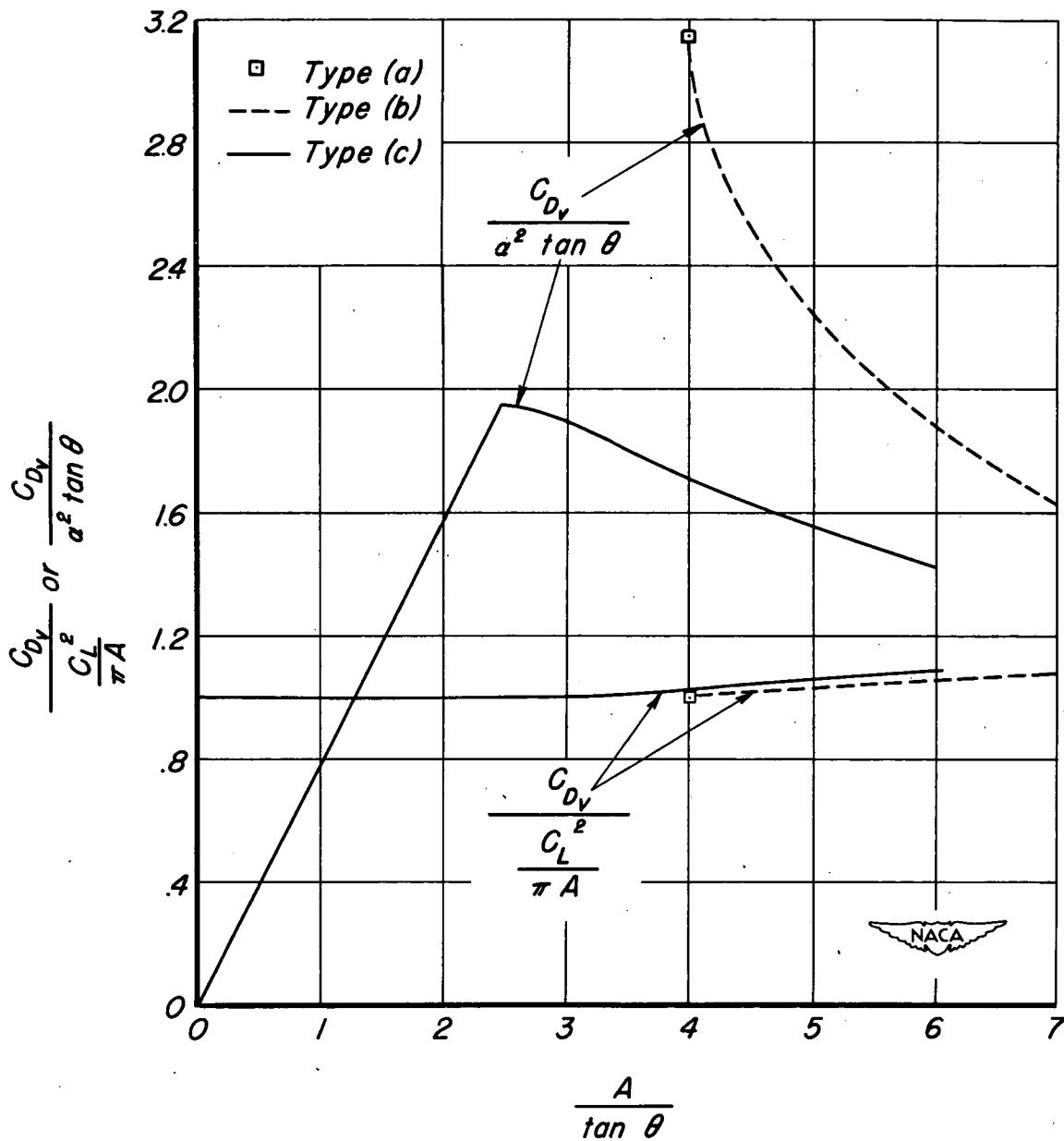
Figure 7.– Variation of lift-curve slope with aspect ratio.

Figure 8.- Variation of vortex drag coefficient with aspect ratio.